Ideal strengths, structure transitions, and bonding properties of a ZnO single crystal under tension

2009 J. Phys.: Condens. Matter 21 495402

(http://iopscience.iop.org/0953-8984/21/49/495402)

J. Phys.: Condens. Matter **21** (2009) 495402 (8pp) doi:10.1088/0953-8984/21/49/495402

Ideal strengths, structure transitions, and bonding properties of a ZnO single crystal under tension

Li-Zhi Xu, Yue-Lin Liu, Hong-Bo Zhou, Li-Hua Liu, Ying Zhang and Guang-Hong Lu

Department of Physics, Beijing University of Aeronautics and Astronautics, Beijing 100191, People's Republic of China

E-mail: LGH@buaa.edu.cn

Received 15 May 2009, in final form 28 September 2009
Published 13 November 2009
Online at stacks.iop.org/JPhysCM/21/495402

Abstract

We perform a first-principles computational tensile test (FPCTT) on a ZnO single crystal based on density functional theory to systematically investigate structural transitions, mechanical, and intrinsic bonding properties in the three representative directions, $[2\bar{1}\bar{1}0]$, [0001], and $[01\bar{1}0]$. Stress as a function of tensile strain shows that the ideal tensile strengths in the three directions are 16.2 GPa, 22.4 GPa, and 19.0 GPa, corresponding to strains of 0.20, 0.16, and 0.16, respectively. The [0001] is the strongest direction due to the strongest bonding between the most closely packed Zn and O(0001) layers. We demonstrate that different structures in these three directions lead to different structural transitions, i.e. from a wurtzite (WZ) to a body-centered tetragonal (BCT) structure for $[2\bar{1}\bar{1}0]$, to a graphite-like (GP-like) structure for [0001], and to a quasi-hexagonal (quasi-HX) structure for $[01\bar{1}0]$, respectively. Bond length and charge density evolution under tension indicate the occurrence of bond formation and disassociation during these structure transitions. New O–Zn bonds form in the WZ → BCT and WZ → quasi-HX transitions, and the original O–Zn bonds break in the WZ → GP-like transition.

(Some figures in this article are in colour only in the electronic version)

1. Introduction

Various properties of a material can be significantly influenced by crystal structures. The polymorphism of crystal structure, which reflects a complex interplay of both intrinsic bonding and extrinsic factors such as applied loading, has long been drawing great research interest. Under extrinsic applied loading, some materials, especially compounds such as ZnO, will exhibit polymorphism and diversity in electronic bonding states [1–5]. It is a remarkable fact that ZnO is considered highly versatile because of not only its inherent semiconductivity at the macroscale, but also its exciting nanoscale properties such as piezoelectricity and pseudoelasticity [1, 6–11]. The mechanical–electrical conversion property of ZnO nanowire has led to the novel invention of nanogenerators for self-powered nanodevices [12, 13]. It has been found that shape memory effects and pseudoelasticity appear in metal nanostructures [14]. Also, differing from the macroscale brittle properties, ZnO exhibits superelasticity in nanostructures such as nanohelices, discovered by Gao *et al* [9]. With the consideration that structure transition plays a key role for both piezoelectric and shape memory effects, it becomes quite important to understand ZnO atomic configuration and intrinsic bonding properties under applied strain.

Typically, the crystal structures shared by ZnO are wurtzite (WZ), zincblende (ZB), and rock salt (RS). WZ is the most stable and commonly observed structure under ambient pressure, while ZB structure can be obtained only on cubic surfaces under specific growth conditions. RS is a structure of a transformation from WZ at relatively high pressures [3, 15, 16]. Recently, both first-principles calculations based on density functional theory (DFT) and molecular dynamics (MD) simulations show that ZnO exhibits a novel hexagonal graphite-like structure in nanostructures [4, 17, 18]. Under extrinsic tensile loading along the $[01\bar{1}0]$ direction, MD simulation indicates that there exists a transition from WZ to a newly discovered hexagonal phase [4, 7]. In addition, the other

properties of ZnO such as band structure and Young's moduli of nanoplates have also been studied computationally [19–21].

The ideal strength of materials is the stress that is required to force deformation or fracture at the elastic instability. The theoretical strength sets an upper bound on the attainable stress. The strength of a real crystal can be changed by the existing cracks, dislocations, grain boundaries, and other microstructural features, but its theoretical value can never be raised. By virtue of the development of the DFT [22, 23] combined with the band-theoretical schemes and the rapid progress of modern computers, recently it became possible to do a first-principles computational tensile test (FPCTT) to investigate the stress–strain relationship and obtain the ideal tensile strength by deforming crystals to failure. Further, it can also predict the structural transition and bonding properties of materials. On the one hand, for single crystals, earlier studies of fcc (Cu, Al, and Ni) and bcc (Mo, W, Nb, and Fe) metals have been performed [24–28]. On the other hand, the effects of impurities Na, Ca, Ga, and S on polycrystalline materials such as an Al grain boundary have also been investigated by the FPCTT [29–32] in order to explore the impurity-induced intergranular embitterment induced by bonding properties.

So far, despite many efforts on ZnO, little has been done on the structural transition, mechanical, and bonding properties in the continuous tensile strain process by the FPCTT. In this paper, we have thus performed the FPCTT on ZnO with a WZ structure to systematically explore the structural transitions, mechanical, and bonding properties in the three representative directions, $[2\bar{1}\bar{1}0]$, [0001], and $[01\bar{1}0]$. Our main focus is to understand the atomic configuration evolution, structure transitions, and bonding properties of ZnO single crystal under tension by performing FPCTT, which can provide useful references for studying the physical and chemical properties of the ZnO polymorphism. The results might also be a reference for the piezoelectric and pseudoelastic behaviors of ZnO that are associated with deformation.

2. Computational method

Our first-principles calculations have been performed using a pseudopotential plane wave method implemented in the VASP code [33, 34] based on the DFT. We used the generalized gradient approximation of Perdew and Wang [35] and projected augmented wave (PAW) potentials [36]. A plane wave energy cutoff of 500 eV was found to be sufficient to converge the total energy and geometry of the WZ structure of ZnO. The equilibrium lattice parameters are calculated for the ZnO single crystal. The a and c are calculated to be 3.28 Å and 5.29 Å, respectively, in good agreement with the corresponding experimental values of 3.25 Å and 5.20 Å. The optimized axis ratio c/a is calculated to be 1.61, consistent with the experimental value of 1.60. It demonstrates accuracy of the employed PAW potentials. The Brillouin zone was sampled with a $4 \times 4 \times 8$ k-point grid according to the Monkhorst–Pack scheme [37] during geometry optimization for an orthorhombic unit cell containing four Zn–O atom pairs. Such a grid was chosen because the change of total energy of the unit cell is less than 0.001 eV with further increasing number of k-points. Both supercell sizes and atomic positions were relaxed to equilibrium, and energy minimization was converged until the forces on all the atoms are less than 10^{-3} eV Å^{-1}.

In the FPCTT, a tensile (uniaxial) strain has been applied to the chosen crystalline direction, and the corresponding stress is calculated according to the Nielsen–Martin scheme [38]. For the uniaxial tensile strain, the tensile stress σ can be calculated from

$$\sigma_{ij} = \frac{1}{\Omega(\varepsilon_{ij})} \frac{\partial E}{\partial \varepsilon_{ij}} \tag{1}$$

where E is the strain energy and $\Omega(\varepsilon_{ij})$ is the volume at a given tensile strain. The lattice vectors are incrementally added in the direction of the imposed stress. At each strain step the structure was relaxed until the stress in the direction orthogonal to the tensile direction vanished, as indicated by those components of the Hellmann–Feynman stresses that are less than 0.1 GPa.

3. FPCTT of zinc oxide in different directions

A uniaxial tensile strain has been applied in the $[2\bar{1}\bar{1}0]$, [0001], and $[01\bar{1}0]$ directions, respectively. An orthorhombic unit cell containing four Zn–O atom pairs extracted from the WZ structure is used in the calculation for all three directions, as shown in figure 1, with lattice parameters of $a = 3.28$ Å, $b = 5.68$ Å, and $c = 5.29$ Å, respectively. Such an orthorhombic unit cell shows sufficient information of the atomic configuration and provides convenience for the simulation of uniaxial tension. In the simulation process, we select the same unit cells (four Zn–O atom pairs) in the different tensile directions.

It can be seen that the nearest neighbor atoms of Zn and O are in different (0001) planes. There exist two kinds of bonds, i.e. the O–Zn bond along the [0001] direction and the inter-plane bond between the two nearest neighbor Zn and O atoms in the neighboring layers. The bond lengths are 2.00 Å and 2.01 Å, respectively, according to the present calculations. Figure 2 shows the strain energy density and the stress as functions of strain in the $[2\bar{1}\bar{1}0]$, [0001], and $[01\bar{1}0]$ directions for the FPCTT.

3.1. FPCTT in the $[2\bar{1}\bar{1}0]$ direction

As shown in figure 1, the $[2\bar{1}\bar{1}0]$ direction corresponds to the orientation between Zn(O) and its nearest neighbor atom in the Zn(O) basal plane. Figure 2 shows the strain energy density and the stress as a function of strain under tensile loading. The strain energy density increases with increasing tensile strain at the beginning, but turns to decrease at a strain of 0.22. It continues to decrease mildly until reaching a local minimum of 0.0129 eV Å^{-3} at a strain of 0.255. The stress as a function of strain increases first but experiences a dramatically drop around the strain of 0.22 from 16.2 GPa to a negative value of −1.6 GPa which is a 'compressive stress'. When the strain reaches 0.255, the stress becomes zero, corresponding to the local minimum of strain energy density. The local minimum of strain energy density and the stress-free state at the strain of 0.255 imply the occurrence of

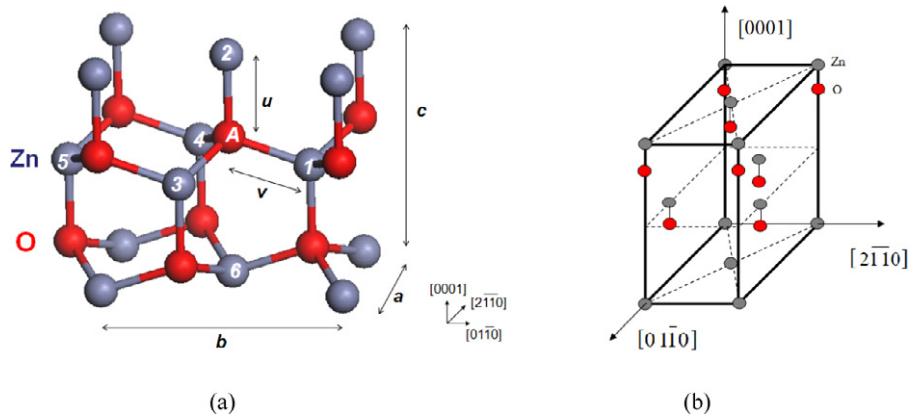

Figure 1. (a) The atomic configuration of the WZ structure. The gray spheres denote Zn atoms, and red spheres denote O atoms. Atoms denoted by A, 1, 2, 3, 4, 5, 6 are for later discussions. (b) The selected unit cell of ZnO with the WZ structure, in which three representative crystalline directions are shown.

a new metastable structure for ZnO. The process between a strain of 0.22 and 0.255 is a spontaneous process, in which the crystal structure automatically transforms to a new atomic configuration (figure 3), because the energy decreases with the strain increasing in this strain range. The 'negative' stress in this strain range is not physically meaningful, and it appears here due to the discontinuous tensile process employed in the present calculations.

Originally, the ZnO crystal is a WZ structure with sixfold symmetry, which can be described as two interpenetrating hcp structures. In the tensile process, with increasing strain, the values of lattice parameters change gradually, as shown in figure 4. In the beginning, lattice parameter a in the [2$\bar{1}\bar{1}$0] direction increases, while b and c in the two directions perpendicular to the tensile direction decrease due to the Poisson effect. When strain rises to 0.22, lattice parameter b suddenly drops, at which point an orthorhombic structure appears. For the initial WZ structure, the 2-A Zn–O pair is in the (01$\bar{1}$0) plane and the 3-A and the 4-A Zn–O pairs are across different (01$\bar{1}$0) planes (figure 1(a)). For this orthorhombic structure, the 3-A and the 4-A Zn–O pairs rotate to enter one single (01$\bar{1}$0) plane in which there also exist 2-A Zn–O pairs, and such a position relationship will not change in subsequent structures. As the strain energy presents a local minimum and the strain–stress curve reaches a stress-free state at a strain of 0.255, the lattice parameter b reaches the same value as a, and the crystal structure exhibits a tetragonal symmetry (figure 3). Energetically such a structure is metastable in comparison with the original sixfold symmetry WZ structure. For both Zn and O atoms in this phase, the crystal lattice can be treated as a body-centered tetragonal (BCT) structure.

We further investigate the bond lengths and charge density distribution of the O–Zn bond in the tensile process. Here we consider five representative O–Zn bonds, i.e. the A-1, A-2, A-3, A-4, and A-5 surrounding the O atom of A, as shown in figure 1(a). Originally, the O–Zn bonds of A-1, A-3, and A-4 are identical due to the sixfold symmetric structure of ZnO, and the corresponding bond lengths are ∼2.00 Å. The O–Zn bond lengths of A-2 and A-5 are ∼2.01 Å and ∼3.84 Å, respectively. Figures 5 and 6 show the change of O–Zn bond length and charge density distribution under the strain in the [2$\bar{1}\bar{1}$0] tensile direction. The A-3 and A-4 bonds are identical in the tensile process due to the symmetry of the crystal structure and the tensile direction, thus we only discuss the bonds of A-1, A-2, A-3, and A-5. As the strain increases, the O–Zn bond length of A-3 increases slowly, and those of A-1 and A-2 remain almost unchanged. In contrast, the bond length of A-5 decreases linearly with increasing strain before the strain of 0.215, and such a phenomenon might be connected with the Poisson effect in the tensile process. After 0.215, the A-5 bond contracts rapidly, while the A-1 bond extends, and the lengths of these two bonds become equivalent at a strain of 0.22. Around this strain point, the sudden shortening of the A-5 distance suggests the formation of a new O–Zn bond. In addition, the charge density distribution (figure 6) also shows a directional covalent bond of A-5 at a strain of 0.22 in comparison with the initial strain-free state. We can thus conclude that such a newly formed O–Zn bond plays a key role in the structure transition from WZ to an unstable orthorhombic structure with a fivefold bonding characteristic. When the strain further increases to 0.255, the A-1, A-3, and A-5 bond lengths become equivalent with a value of ∼2.12 Å, larger than their original lengths, while the A-2 bond length is 2.03 Å, corresponding to a stress-free metastable BCT structure. Therefore, the structure transitions are from the initial WZ structure to a BCT compound structure via the unstable orthorhombic structure during the [2$\bar{1}\bar{1}$0] tensile process.

3.2. FPCTT in the [0001] direction

The [0001] direction is the most symmetric path for ZnO, and the sixfold symmetry remains unchanged in the tensile process. As shown in figure 1, in the beginning, the strain energy density as a function of strain increases nearly quadratically, leading to a linear-like increase of the stress. However, when the strain ranges from 0.16 to 0.20, the stress decreases dramatically from a maximum of 22.4–6.1 GPa. The energy density changes correspondingly.

As shown in figure 7, a new GP-like structure occurs at a strain of 0.20. Originally, the Zn and O atoms are in different

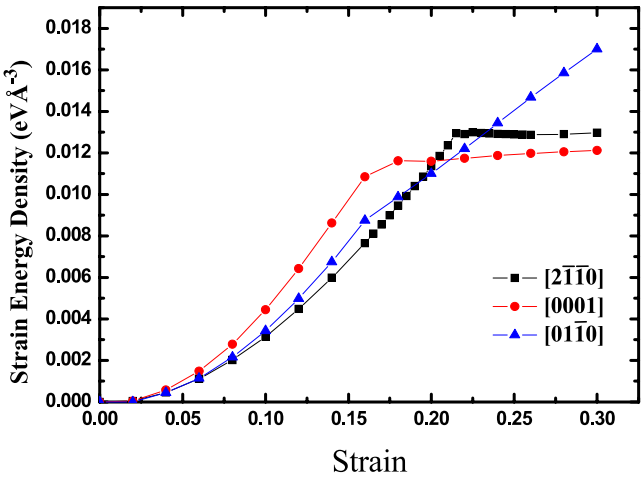

(a)

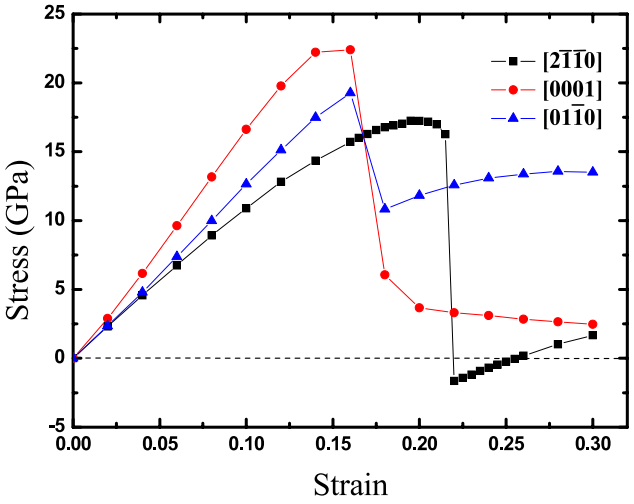

(b)

Figure 2. The strain energy density (a) and stress (b) of a ZnO tensile unit cell as a function of uniaxial deformation in the [2$\bar{1}\bar{1}$0], [0001], and [01$\bar{1}$0] directions.

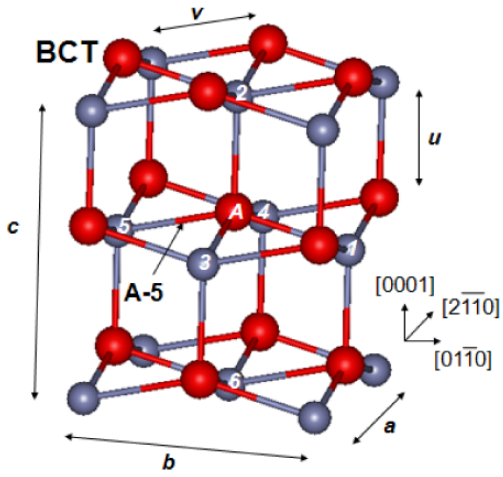

Figure 3. BCT structure occurs at a strain of 0.255 in the [2$\bar{1}\bar{1}$0] direction.

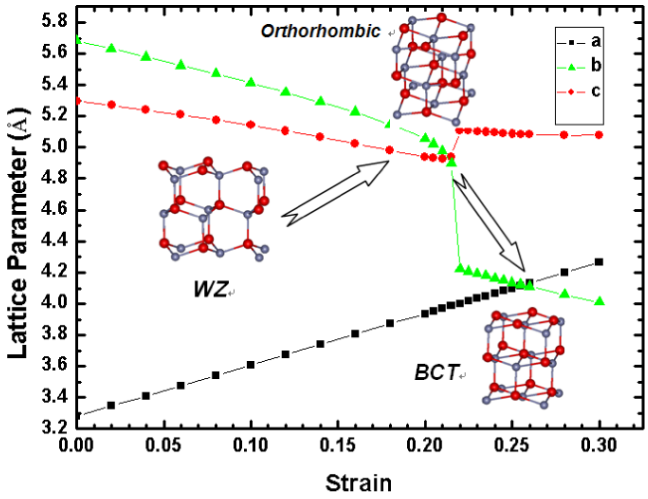

Figure 4. The evolution of lattice parameters and geometric structures as a function of tensile strain in the [2$\bar{1}\bar{1}$0] direction. The structure evolves as WZ → orthorhombic → BCT, as shown in the three inset panels.

(0001) planes. When the strain ranges from 0.18 to 0.20, these Zn and O atoms become coplanar, characterized by the formation of Zn–O hexatomic rings. Such a structure is GP-like with hexagonal symmetry.

We now turn to discuss the bond lengths as a function of strain, as shown in figure 8. Here we consider five representative O–Zn bonds, i.e. A-1, A-2, A-3, A-4, and A-6 surrounding the O atom of A, as shown in figure 8. The lengths of A-1 and A-3 remain equivalent to each other and change little with the increasing strain. However, when the strain is beyond 0.16, A-2 extends rapidly, and exhibits an equivalent length with A-6 at a strain of 0.22. This suggests that the break of the A-2 bond occurs here. Corresponding to the changes in bond lengths, figure 9 shows the charge density distribution under different strain. The charge density on the (2$\bar{1}\bar{1}$0) plane shows a dramatic decrease between Zn atom 2 and O beyond 0.16, implying such a bond break, consistent with the bond length evolution results. The charge density on the (0001) plane shows covalent bonding characteristics among the hexatomic rings in the Zn–O coplanar layer. With further strain increase, the A-2 and A-6 bond lengths increase linearly, while the A-1 and A-3 bonds remain almost unchanged.

Thus, it is clear that the structure transition from the WZ to the GP structure in the [0001] direction is characterized by the break of the O–Zn bond (A-2) along the [0001] direction. The stress under the [0001] direction elongates the (0001) face distance, leading to the [0001]-oriented O–Zn bond break. This makes the structure quite similar to the graphite, which exhibits the van der Waals weak interaction between the graphite layers, but bonds covalently inside the layers.

3.3. FPCTT in the [01$\bar{1}$0] direction

Figure 2 shows strain energy density and stress as a function of strain in the [01$\bar{1}$0] direction. The strain energy density increases initially with increasing strain, and its slope

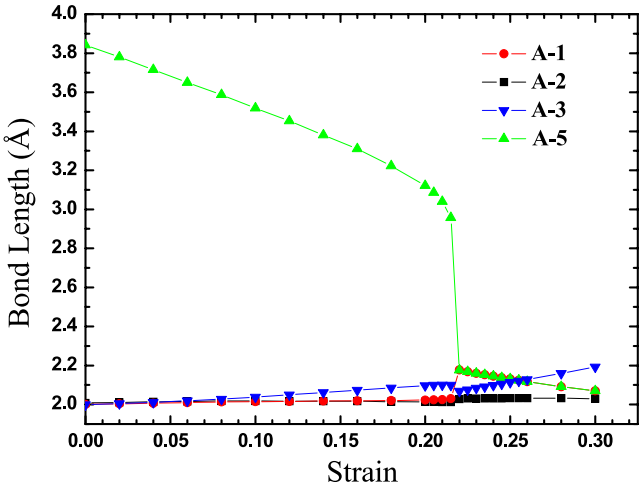

Figure 5. The length evolution of representative bonds with increasing strain under a uniaxial tensile strain applied in the [$2\bar{1}\bar{1}0$] direction.

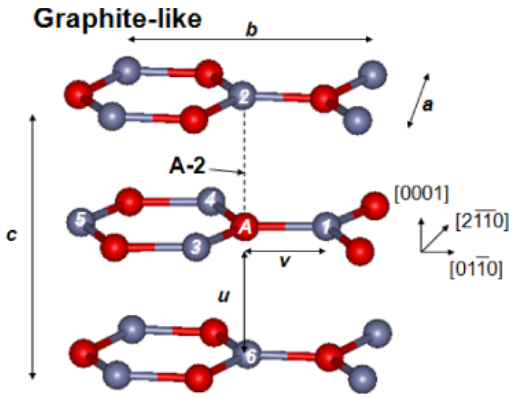

Figure 7. Graphite-like structure beyond a strain of 0.20 in the [0001] direction.

decreases from a strain of 0.16. Correspondingly, the stress exhibits a maximum of 19.3 GPa at 0.16. At a strain of 0.18, the stress decreases quickly to 10.8 GPa.

Similar to the structural transition in the [0001] direction, the Zn and O atoms, which are initially in different (0001) neighboring planes, turn into the same (0001) plane and form hexatomic rings beyond a strain of 0.18. A quasi-hexagonal (quasi-HX) structure forms, as shown in figure 10. In comparison with the ideal HX structure, the bond angles (α_1 and α_2) in the hexatomic rings in the quasi-HX structure are not strictly equal to 120°. These two angles are 106.0° and 127.0°, respectively. Figure 11 shows that the bond lengths of A-1 and A-3 (symmetrically identical to A-4) increase along the tensile direction. The A-6 length is suddenly shortened from 2.89 Å to 2.15 Å from the strain of 0.16 to 0.18. The charge density evolution clearly shows a newly formed A-6 bond (figure 12). The charge density on the ($2\bar{1}\bar{1}0$) plane shows a dramatic increase between Zn atom 6 and O beyond 0.16 containing covalent bonding components. The charge density on the (0001) plane shows a similar characteristic among the hexatomic rings in the Zn–O coplanar layer.

We can thus understand that the WZ structure of ZnO is compressed in the direction normal to the [$01\bar{1}0$] direction due to the Poisson effect under the tension in [$01\bar{1}0$]. Due to such compression, the Zn and O atoms in different ($01\bar{1}0$) neighboring planes become coplanar. Moreover, a new A-6 covalent bond is formed between the layers. On the other hand, elongation in [$01\bar{1}0$] makes the configuration deviate from the originally hexagonal one. These originate the structure transition from WZ to quasi-HX.

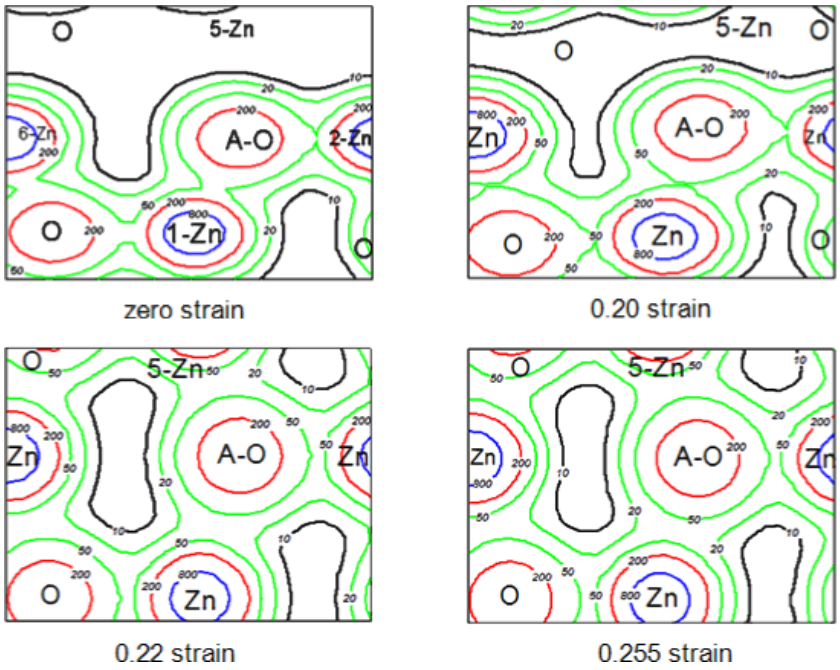

Figure 6. The evolution of the charge density distribution of O–Zn bonds in the ($2\bar{1}\bar{1}0$) plane at different strain values.

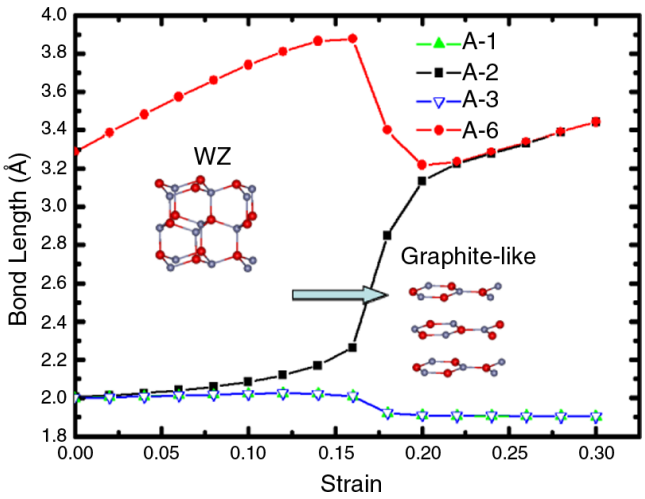

Figure 8. Bond length evolution of the representative bonds with increasing strain under a uniaxial tensile strain in the [0001] direction. The inset panels show the structure configurations in the different strain ranges.

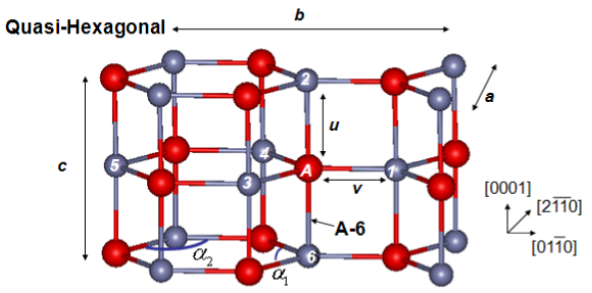

Figure 10. Quasi-hexagonal structure occurs at a strain of 0.18 in the [01$\bar{1}$0] direction.

Table 1. Structural transitions, stress maxima and the corresponding strains in the present FPCTT.

	FPCTT		
Directions	Structure transitions	Stress (GPa)	Strain
[2$\bar{1}\bar{1}$0]	WZ → BCT	16.2	0.20
[0001]	WZ → GP-like	22.4	0.16
[01$\bar{1}$0]	WZ → quasi-HX	19.0	0.16

4. Comparison of three tensile directions and with other computational work

The present FPCTT indicates totally different structure transitions in the three different tensile directions. Under tension, the [2$\bar{1}\bar{1}$0], [0001], and [01$\bar{1}$0] directions exhibit structure transitions from WZ to BCT, GP-like, and quasi-HX structure, respectively. The corresponding strains are 0.255, 0.20, and 0.18, respectively. These structural transitions, the corresponding stress maxima and strains are listed in table 1. For the present FPCTT, we observe a GP-like structure with the Zn and O atoms in the same (0001) plane, and this structure has also been observed in previous simulations of ZnO nanostructures [4, 17, 18].

The [0001] direction can be considered as the strongest direction with the ideal strength as large as ∼22.4 GPa, while the [2$\bar{1}\bar{1}$0] and [01$\bar{1}$0] directions are weaker with ideal strengths of ∼16.2 GPa and ∼19.0 GPa, respectively. This can be understood as the (0001) plane being the most closely packed crystalline plane in ZnO in comparison with other planes such as (2$\bar{1}\bar{1}$0) and (01$\bar{1}$0), leading to the strongest interaction between the neighboring Zn and O atoms between the (0001) planes.

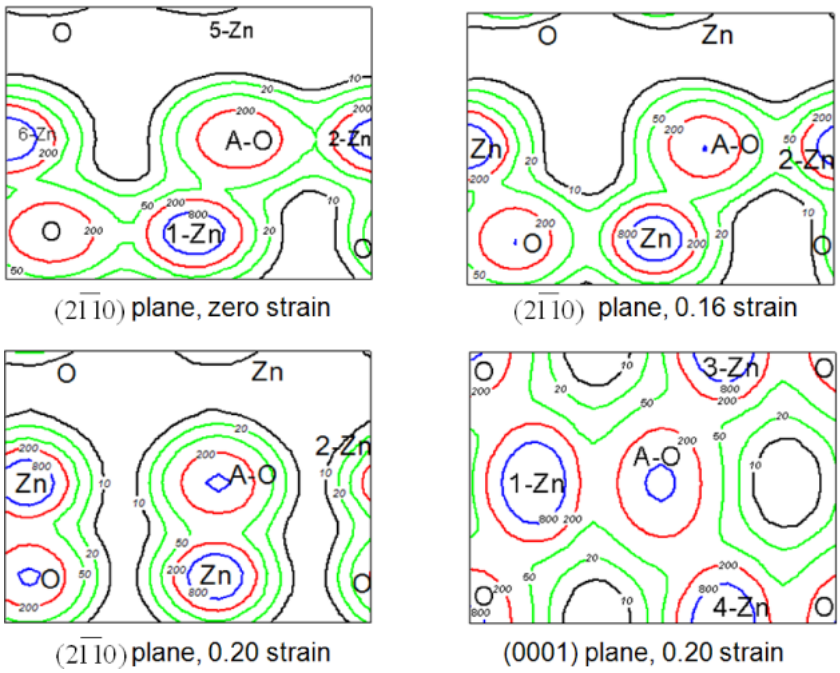

Figure 9. Charge distribution evolution of O–Zn bonds in the tensile process along [0001].

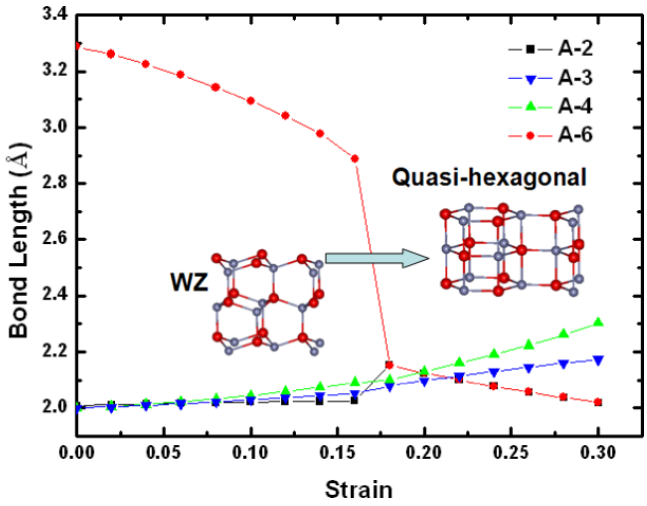

Figure 11. The length evolution of the representative bonds with increasing strain under a uniaxial tensile strain applied in the $[01\bar{1}0]$ direction. The inset panels show the structure configurations in the different strain ranges.

Kulkarni *et al* investigated the structural transitions in the ZnO nanowire/nanorod under tensile loading in the $[2\bar{1}\bar{1}0]$, [0001], and $[01\bar{1}0]$ directions using an MD method [1, 39]. The lateral dimensions of the nanowire/nanorod are ∼20 Å × 20 Å, and the temperature varies from 100 to 1200 K. The results show that the [0001] direction exhibits the largest tensile strength as compared with the other directions. For the $[2\bar{1}\bar{1}0]$ tensile direction, a transition from WZ to HX structure appears. For the [0001] tensile direction, a BCT structure with four-atom rings (BCT-4) forms, and the corresponding breaking and recombination of O–Zn bonds was reported as well. For the $[01\bar{1}0]$ tensile direction, a transition from WZ to HX occurs. As a matter of fact, the present FPCTT cannot directly compare with the MD simulations, because the structure transitions of ZnO nanowire/nanorod under tension have been performed in MD instead of the periodical single crystal used in the present FPCTT. However, we can still find some structural similarity under tension in both simulations. For example, the fivefold coordination characteristic and the formation of the O–Zn bond (A-6 in the present FPCTT) have been observed in both MD and FPCTT.

5. Summary

We have performed a FPCTT on a ZnO single crystal based on density functional theory to systematically investigate structural transitions, mechanical behaviors, and intrinsic bonding properties in the three representative directions, $[2\bar{1}\bar{1}0]$, [0001], and $[01\bar{1}0]$. The ideal tensile strengths in the three directions are 16.2 GPa, 22.4 GPa, and 19.0 GPa, corresponding to strains of 0.20, 0.16, and 0.16, respectively. The [0001] is the strongest direction in comparison with $[2\bar{1}\bar{1}0]$ and $[01\bar{1}0]$, originating from the strongest bonding between the most closely packed Zn and O(0001) layers. The three directions exhibit different structural characteristics, leading to different structural transitions under tension, which are from a WZ to a BCT structure for $[2\bar{1}\bar{1}0]$, from WZ to a GP-like structure for [0001] and from WZ to a quasi-HX structure for $[01\bar{1}0]$, respectively. The GP-like structure has also been observed in the previous simulation work. These structure transitions stem from the bond formation and dissociation, including the formation of new O–Zn bonds in the WZ → BCT and WZ → quasi-HX structural transitions, and the breaking of the O–Zn bond in the WZ → GP-like structural transition.

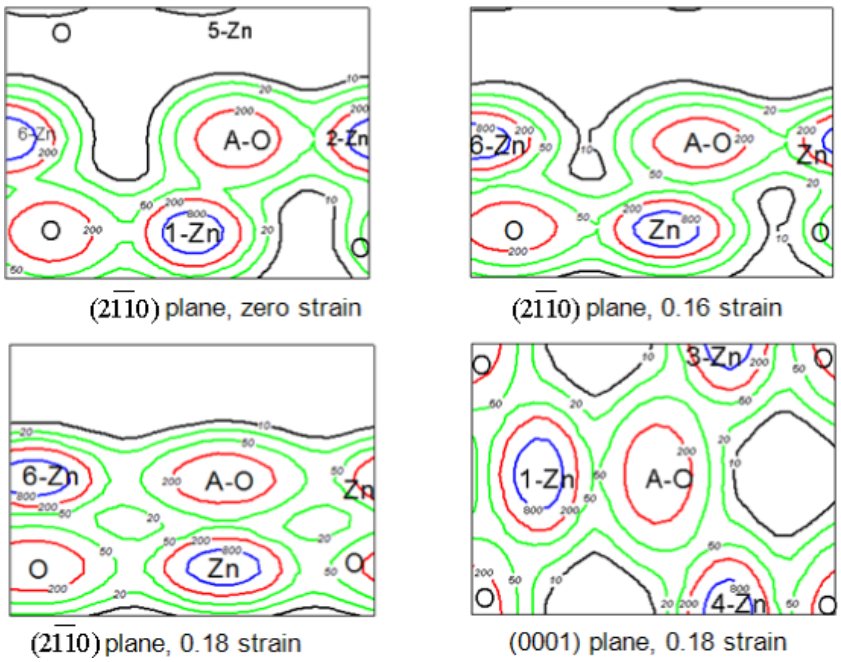

Figure 12. The evolution of charge density distribution of O–Zn bonds in representative planes at different strains.

References

[1] Kulkarni A J, Zhou M, Sarasamak K and Limpijumnong S 2006 *Phys. Rev. Lett.* **97** 105502
[2] Bates C H, White W B and Roy R 1962 *Science* **137** 993
[3] Ozgur U, Alivov Y I, Liu C, Teke A, Reshchikov M A, Dogan S, Avrutin V, Cho S J and Morkoc H 2005 *J. Appl. Phys.* **98** 041301
[4] Wang B, Zhao J, Jia J, Shi D, Wan J and Wang G 2008 *Appl. Phys. Lett.* **93** 021918
[5] Kulkarni A J and Zhou M 2008 *J. Mech. Phys. Solids* **56** 2473
[6] Wang Z L 2004 *J. Phys.: Condens. Matter* **16** 829
[7] Kulkarni A J and Zhou M 2006 *Acta Mech. Sin.* **22** 217
[8] Kulkarni A J, Zhou M and Ke F J 2005 *Nanotechnology* **16** 2749
[9] Gao P X, Mai W and Wang Z L 2006 *Nano Lett.* **6** 2536
[10] Zhou J, Fei P, Gao Y, Gu Y, Liu J, Bao G and Wang Z L 2008 *Nano Lett.* **8** 2725
[11] Wang Z L 2007 *Adv. Mater.* **19** 889
[12] Wang Z L and Song J 2006 *Science* **312** 242
[13] Qin Y, Wang X and Wang Z L 2008 *Nature* **451** 809
[14] Park H S, Gall K and Zimmerman J A 2005 *Phys. Rev. Lett.* **95** 255504
[15] Limpijumnong S and Lambrecht W R L 2001 *Phys. Rev. Lett.* **86** 91
[16] Jaffe J E, Snyder J A, Lin Z and Hess A C 2000 *Phys. Rev.* B **62** 1660
[17] Zhang L and Huang H 2007 *Appl. Phys. Lett.* **90** 023115
[18] Freeman C L, Claeyssens F, Allan N L and Harding J H 2006 *Phys. Rev. Lett.* **96** 066102
[19] Zhou G C, Sun L Z, Zhong X L, Chen X, Wei L and Wang J B 2007 *Phys. Lett.* A **368** 112
[20] Zhang L and Huang H 2006 *Appl. Phys. Lett.* **89** 183111
[21] Zahn D 2008 *J. Chem. Phys.* **128** 184707
[22] Hohenberg G P and Kohn W 1964 *Phys. Rev.* **136** B864
[23] Kohn W and Sham L J 1965 *Phys. Rev.* **140** A1133
[24] Luo W, Roundy D, Cohen M L and Morris J W Jr 2002 *Phys. Rev.* B **66** 094110
[25] Roundy D, Krenn C R, Cohen M L and Morris J W Jr 1999 *Phys. Rev. Lett.* **82** 2713
[26] Ogata S, Li J and Yip S 2002 *Science* **298** 807
[27] Clatterbuck D M, Chrzan D C and Morris J W Jr 2003 *Acta Mater.* **51** 2271
[28] Liu Y L, Zhang Y, Zhou H B, Lu G H and Kohyama M 2008 *J. Phys.: Condens. Matter* **20** 335216
[29] Lu G H, Deng S H, Wang T M, Kohyama M and Yamamoto R 2004 *Phys. Rev.* B **69** 134106
[30] Zhang Y, Lu G H, Wang T M, Deng S H, Kohyama M and Yamamoto R 2006 *Mater. Trans.* **47** 2678
[31] Lu G H, Zhang Y, Deng S H, Wang T M, Kohyama M, Yamamoto R, Liu F, Horikawa K and Kanno M 2006 *Phys. Rev.* B **73** 224115
[32] Zhang Y, Lu G H, Deng S H, Wang T M, Xu H B, Kohyama M and Yamamoto R 2007 *Phys. Rev.* B **75** 174101
[33] Kresse G and Hafner J 1993 *Phys. Rev.* B **47** 558
[34] Kresse G and Furthmüller J 1996 *Phys. Rev.* B **54** 11169
[35] Perdew J P and Wang Y 1992 *Phys. Rev.* B **45** 13244
[36] Blochl P E 1994 *Phys. Rev.* B **50** 17953
[37] Monkhorst H J and Pack J D 1976 *Phys. Rev.* B **13** 5188
[38] Nielsen O H and Martin R M 1987 *Phys. Rev.* B **32** 3780
[39] Wang J, Kulkarni A J, Sarasamak K, Limpijumnong S, Ke F J and Zhou M 2007 *Phys. Rev.* B **76** 172103